STRENGTH LOSS AND HAZARD ASSESSMENT OF EUPHRATES POPLAR USING STRESS WAVE TOMOGRAPHY

Shanqing Liang
Research Assistant
E-mail: liangsq@caf.ac.cn

*Feng Fu**
Professor
Research Institute of Wood Industry
Chinese Academy of Forestry
Beijing, China 100091
E-mail: feng@caf.ac.cn

(Received June 2011)

Abstract. Stress wave tomography is a noninvasive testing method for diagnosing defects in standing or cut trees. For this study, the technique was used to diagnose defects on 15 disks of Euphrates poplar (*Poulus euphratica* Oliv.) cross-sections. Two-dimensional tomograms were generated and used to estimate strength loss and assess potential tree stem failures. Results found that stress wave tomograms can effectively locate decay and void dimensions and that there was a logarithmic significant relationship ($r = 0.9679$) between real tomographic defect areas and visual defect areas indicated by the tomograms. This regression relationship could improve accuracy of hazard assessment in historic trees when using stress wave tomography. Strength loss was calculated based on Wagener, Coder, and Mattheck's equations. These three equations can provide effective internal tree stem weakness assessment. However, strength loss between tomographic defect areas in cross-sections and real visual defect area had a significant 0.05 statistical difference. The results of this study provided insight into defect diagnosis and hazard assessment for trees in China, especially those with historical significance.

Keywords: Stress wave tomography, defect, strength loss, hazard assessment.

INTRODUCTION

Stability of urban trees is a major concern to public safety in cities and urban communities. Tree decay detection has been researched using stress wave tomography by arborists and wood scientists around the world (Maurer et al 2002; Glibert and Smiley 2004; Wang et al 2009). Most tree stems in China that fall into the historic and famous category contain decay, hollow areas, and cracks because of their age. These various internal defects can result in tree failure and tree mortality causing significant loss in traditional historical culture. To protect public safety and preserve these historic and famous trees, arborists need advanced nondestructive testing tools to detect internal defects and assess any potential. Decay, hollow areas, and cracks in tree stems can lead to inner strength loss that ultimately affects tree stability. It is a big challenge for arborists to accurately assess potential hazards from historic trees using stress wave tomography (Allison et al 2008). Stress wave tomography is based on stress wave transmission in wood and coupled with computer tomography techniques. It produces stress-wave-based tomograms that reflect internal tree stem condition. Tomograms, as a means of urban tree hazard assessment, have been investigated in recent years (Comino et al 2000; Divos and Szalai 2002; Wang et al 2005; Fink and Schwarze 2008). In China, historic trees need more stress wave tomography research to provide insight and guidelines for detecting internal defects and assessing hazard posed by historic trees.

The objective of this study was to determine failure risk of Euphrates poplar (*Poulus*

* Corresponding author

© 2012 by the Society of Wood Science and Technology

euphratica Oliv.) with decay and cavities using stress wave tomography to estimate strength loss and resulting potential hazards to property and people. To accomplish this, strength loss and assessment equations were discussed, and a relationship model was developed to calculate defect dimensions with respect to measured dimensions. Data were then used to quantitatively analyze actual tree defect dimensions (eg, decay, void, hollows, and cracks) using equations developed by Wagener, Coder, and Mattheck to assess tree stem hazards according to tomographic defect areas and real visual defect areas.

MATERIALS AND METHODS

Disk Samples

Fifteen Euphrates poplar logs were harvested in Ejna Banner, Inner Mongolia. The trees were praised as "heroic desert trees" in China. Fifteen 100-mm-thick disks were cut from the logs (diameters of 293, 207, 345, 283, 299, 329, 280, 302, 236, 313, 370, 226, 383, 374, and 283 mm) to be used as tomogram test samples. All selected disks exhibited decay or voids. Three healthy logs (1.5 m long) and five logs with decay or voids (1.5 m long) were selected to have small specimens cut from them for measuring density, modulus of elasticity (MOE), bending strength, and toughness. The other seven logs could not be used for making specimens because of severe decay or large voids.

Tomogram

The disks were tested using an Arbotom acoustic tomography tool (Rinntech, Heidelberg, Germany) with 12 sensors for detecting inner structural defects. In each tomography test, we used 12 sensors to measure transit times through multiple paths. All sensors were spaced at 30° intervals around the periphery, and each position was pulsed sequentially to generate stress waves traveling through the wood. The time the stress wave traveled between 11 sensors was recorded and transferred into velocities (Fig 1). A stress wave two-dimensional tomogram was generated for each disk using Rinntech Arbotom software. Disk moisture content was measured using a CSA electronic moisture meter (Model Delta-55; CSA electronic Meß- und Regelgeräte GmbH, Freiberg, Germany). After laboratory testing, all disks were photographed for visually determining and calculating defect areas.

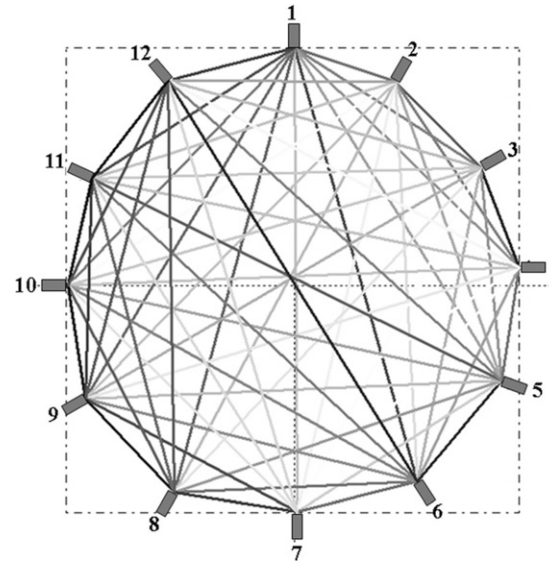

Figure 1. Diagram of 12 sensors located around the periphery with Rinntech Arbotom tomography tool.

Mechanical Properties of Wood

MOE, bending strength, and toughness were tested in this study. The test standards for baseline measurements were as follows: MOE—in accordance with Method for Determination of the Modulus of Elasticity in Static Bending of Wood (Chinese National Standard [CNS] 2009a), bending strength—in accordance with Method of Testing in Bending Strength of Wood (CNS 2009b), and toughness—in accordance with Method of Testing in Toughness of Wood (CNS 2009c). These three mechanical properties were compared between healthy and unhealthy wood.

Data Processing and Statistical Analysis

Assessment equations of Wagener, Coder, Fraedrich, and Mattheck need to measure the diameter of decay and void to calculate strength loss. However, decay and void in tree stems are irregular shapes. For more accurately obtaining average diameter of decay and void, four directions (east–west, south–north, southeast–northwest, and northeast–southwest) were selected on the disks and tomograms to calculate average diameter using SigmaScan Pro.5 software (Systat Software Inc, San Jose, CA). Defect areas shown on the tomograms and disks were calculated using the same software. Area calculation with the software was based on the following procedure: 1) calculate pixel value per 10-mm length to get pixel value of 10-mm^2 area; 2) use a trace code option to calculate a pixel of the defect area; and 3) total pixel of the defect area was divided by the pixel value of 10-mm^2 area to give the value of the defect area. Diameter and defect area were used to assess tree stem risk in combination with equations from Wagener, Coder, and Mattheck's research results. A 0.05 significance level was used in statistically analyzing values between the tomograms and actual disks.

RESULTS AND DISCUSSION

Tomogram Assessment

Potential tree failure is very high when decay, hollow areas, cracks, and void exist in tree stems. However, a tree is a living organism and many factors influence failures such as condition, age, wind, etc, making it difficult to predict when a tree will fail. Some prediction equations have been developed, including those by Wagener, Coder, Fraedrich, and Mattheck. Table 1 shows four equations and hazard thresholds (Wagener 1963; Coder 1989; Smiley and Fraedrich 1992; Mattheck and Breloer 1994).

Four equations were used to assess tree stem failure risk. Mattheck's equation focuses on the decay center and the stem's center not being in the same location, but Wagener's, Coder's, and Fraedrich's equations are all based on decay and cross-section having the same center. As seen in the 15 tomograms, the color changes from dark gray to light gray when the wood changes from sound areas to decayed or void areas. The line is the area in which Mattheck's equation indicates the assessment reference value using a 0.3 hazard threshold (Fig 2). Tree stem was assessed as being at the risk level if the decay area was larger than the gray line area. This method can provide fast assessment results for researchers, but the defect area must be accurately calculated so that the difference is decreased when comparing defect area with area calculated by the hazard threshold.

Figure 2 shows 15 Euphrates poplar cross-section tomograms. Most of the tomograms show decay or void areas in the disks. Disk numbers 1-4, 7, 13, 14, and 15 have significant dark areas indicating severe decay or void areas detected by stress wave tomography. Other tomograms also found decay but the light gray area is not significant enough to diagnose the extent of the decay. Although stress wave tomography does not identify defect types in the tree stems, it still provides excellent information for tree defect diagnosis and risk assessment. In all tomograms, the gray line is 0.3 threshold (t/R = 0.3) hazard assessment based on Mattheck's equation (Mattheck and Breloer 1994). The tree stem will be assessed in the hazard level if the area of decay is larger than the inner area of the gray line.

Table 1. Assessment threshold of four equations.[a]

Item	Wagener (%)	Coder (%)	Fraedrich (%)	Mattheck
Equation	d^3/D^3	d^4/D^4	$(d^3+R(D^3-d^3))/D^3$	t/R
Hazard threshold	33%	$20\% \leq I \leq 44\%$ (caution) $>44\%$ (danger)	33%	0.3

[a] Where d is the diameter of the decay column; D is the average stem diameter inside the bark; R is the ratio of cavity opening to stem circumference (Fraedrich's); t is the thickness of sound wood remaining in the stem; R is the stem radius (Mattheck's).

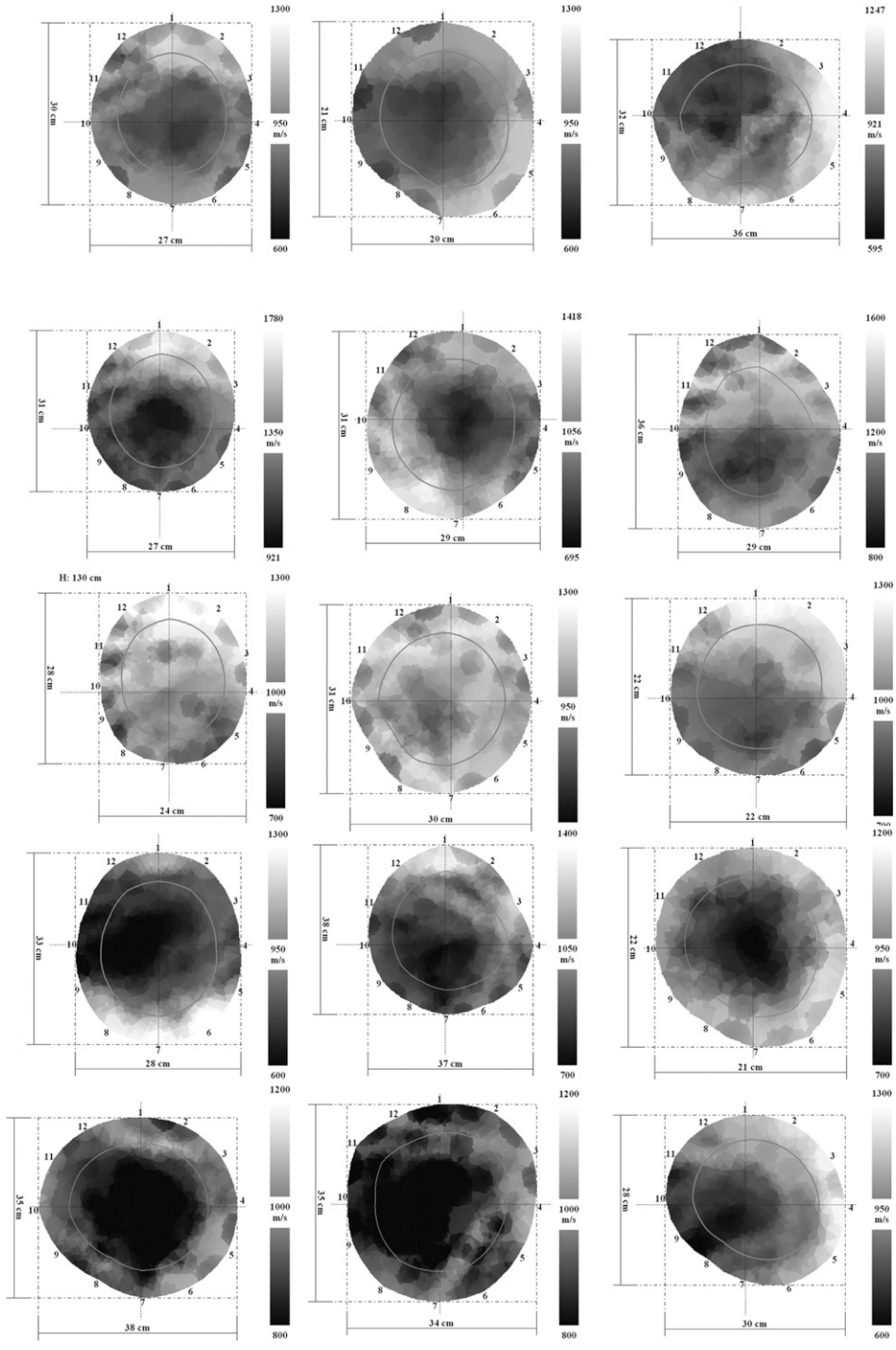

Figure 2. Two-dimensional tomograms from disks 1 to 15. Gray line in tomogram is hazard assessment at 0.3 threshold (t/R = 0.3) from the Mattheck equation (Mattheck and Breloer 1994).

Strength Loss and Hazard Assessment

Table 2 shows that density, MOE, bending strength, and toughness values of healthy wood were higher than in wood with defects. Values for healthy wood were 523-544 kg/m^3, 57.9-68.3 MPa, 4.4-4.7 MPa, and 34.6-39.6 kJ/m^2, respectively, which is a 11.4, 19.5, 14.3, and 22.9% ratio difference. The unhealthy wood (decay and voids) values were 433-516 kg/m^3, 39.9-57.1 MPa, 3.3-4.6 MPa, and 20.3-38.2 kJ/m, respectively (Table 2). Test results showed that mechanical properties from wood with defects were all lower than for sound wood. However, in a tree stem, mechanical properties need to be estimated by nondestructive testing and a calculation equation. Table 3 shows estimated strength loss in 15 disks when calculated using Wagener, Coder, and Mattheck equations. Fraedrich's equation was not used to calculate strength loss because it only applies to open cavities, and there were no open cavities in the disks in this study. In Table 4, disks 1, 3, and 10-15 were assessed at the danger, or caution, level based on the hazard threshold. The other disks were rated as safe. Strength loss results also showed that decay or void areas existed in these disks.

Combined with strength loss equations, stress wave tomography can effectively detect internal defects and provide quantitative analysis of stability trees. When strength loss of the real disks was compared with that of the tomograms, Wagener's equation showed a better match than

Table 2. Mechanical properties of healthy wood and wood with defects.

Log no.	Wood condition	Density (kg/m^3)	Modulus of elasticity (MPa)	Bending strength (MPa)	Toughness (kJ/m^2)
1	Healthy	523	57.9	4.4	39.6
2	Healthy	571	68.3	4.6	35.3
3	Healthy	544	66.7	4.7	34.6
4	Decay	433	57.1	4.2	38.2
5	Decay	479	53.1	4.3	30.5
6	Void	516	54.2	3.6	27.4
7	Void	479	55.0	4.6	24.2
8	Void	513	39.3	3.0	20.3
Total mean of healthy wood		546	64.32	4.59	36.50
Total mean of decay and void wood		484	51.75	3.93	28.12
Ratio difference between healthy and unhealthy wood (%)		11.4	19.5	14.3	22.9

Table 3. Estimated strength loss of real disk and tomograms tested by different equations.

	Strength loss derived from tomogram			Strength loss derived from disk		
Disk no.	Wagener (%)	Coder (%)	Mattheck	Wagener (%)	Coder (%)	Mattheck
1	45.8	36.2	0.1	55.0	45.2	0.2
2	8.2	3.7	0.3	9.1	4.1	0.6
3	45.0	35.8	0.1	42.9	34.9	0.3
4	1.3	0.3	0.5	1.4	0.4	0.7
5	6.2	2.5	0.3	6.1	2.7	0.6
6	2.7	0.8	0.4	2.1	0.6	0.7
7	10.5	5.0	0.3	10.5	5.0	0.5
8	2.7	0.9	0.4	3.7	1.2	0.7
9	2.7	0.9	0.5	2.9	1.3	0.8
10	39.4	29.1	0.2	53.1	44.8	0.2
11	41.1	31.3	0.1	33.6	23.8	0.3
12	35.0	24.7	0.2	35.6	25.2	0.3
13	49.8	39.7	0.1	52.6	42.5	0.2
14	52.2	42.5	0.1	55.1	45.1	0.2
15	45.0	35.1	0.2	47.4	37.0	0.2

Table 4. Tree trunk hazard assessment results by different assessment equations.

	Wagener			Coder			Mattheck		
Disk no.	Tomo[a]	Real[b]	Pre (%)[c]	Tomo	Real	Pre (%)	Tomo	Real	Pre (%)
1	**[d]	**	100	**	**	100	**	**	100
2	**	—	0	—	—	100	*	—	50
3	**	**	100	**	**	100	**	*	50
4	—	—	100	—	—	100	—	—	100
5	—	—	100	—	—	100	*	—	50
6	—	—	100	—	—	100	—	—	100
7	—	—	100	—	—	100	*	—	50
8	—	—	100	—	—	100	—	—	100
9	—	—	100	—	—	100	—	—	100
10	**	**	100	*	**	100	**	**	100
11	**	**	100	*	*	100	**	*	50
12	**	**	100	*	*	100	**	*	50
13	**	**	100	*	*	100	**	**	100
14	**	**	100	*	**	50	**	**	100
15	**	**	100	*	*	100	**	**	100

[a] Tomogram hazard assessment.
[b] Disk hazard assessment.
[c] Assessment precision between tomogram and disk.
* Caution level; ** danger level; — safe level.

did the other equations. However, Wagener's hypothesis states that the decay and the stem share the same geometric center. The assessment result would be significantly different if the decay area center was not the same as the stem center because the decay diameter shown by the tomogram would be less than the real dimension, which potentially could lead to hazard underestimation. Coder's equation is based on the strength loss formula of a cylinder, therefore the equation is not concerned about the different geometric center between decay area and stem. Mattheck's equation is based on buckling strength of a cylinder, hence it also offers a measure of stem failure probability and is concerned about the center of the defect and stem. Therefore, Mattheck's equation is better for assessing decay that does not share the same center with the stem. There is a clear difference in estimated strength loss between a tomogram and the disk calculations when using Wagener's equation. Disks 3, 5-7, and 11 show that strength losses estimated from tomograms were greater than those estimated from the disk. With Coder's equation, estimated strength loss from the tomograms of disks 3, 6, and 11 was greater than that from the disks. For the remaining disks, however, estimated strength loss was greater from the disks than the tomograms. However, all strength loss from the tomograms was less than from the disks using Mattheck's equation.

Statistical analysis of strength loss indicates that there is a significant difference at the 0.05 level between the tomograms and the disks (Table 5). To decrease tomogram strength loss prediction error, more sensors should be used for the test. Based on laboratory results and analysis, the Wagener, Coder, and Mattheck equations can be used to assess tree stem strength loss when decay and void areas share the same center with stem. Mattheck's equation should be used to assess strength loss if the defect center is different from the stem center. In the case of open cavities, it is better to use Fraedrich's equation.

Relationship Model

Model introduction. Results for determining tree stem mechanical properties using nondestructive methods were affected by various factors including materials, sensor configuration, instruments, and defect locations. With stress wave tomography, defect areas shown by tomograms were different compared with the actual

Table 5. Strength loss analysis of variance between tomograms and disks.

Equation type	Difference source	Sum of squares	Degree of freedom	Mean square	F value	Significance
Wagener	Between groups	7111.32	11	646.48	170.05	0.0001**
	Within groups	11.41	3	3.82		
	Total	7122.72	14			
Coder	Between groups	5166.88	13	397.45	79490.45	0.003**
	Within groups	0.005	1	0.005		
	Total	5166.88	14			
Mattheck	Between groups	0.70	4	0.18	57.94	0.0001**
	Within groups	0.03	10	0.003		
	Total	0.73	14			

** Significantly different at the 0.05 level.

stem cross section. However, the tomogram defect area can be more accurately calculated through a relationship model between the tomogram defect area and the actual disk. The model can be calculated according to the following formula (Fu and Liu 1999):

$$\varphi(a) = \lambda_0 + \lambda_1\varphi(a') + \lambda_2\varphi^2(a') + \ldots + \lambda_m\varphi^m(a') + \varepsilon\ \varepsilon \sim N(0, \sigma^2) \quad (1)$$

where $\varphi(\cdot)$ is the mathematical function, λ_i, i = 0, 1, 2,. . ., m, and σ^2 are uncertainty parameters from regression analysis methods. In the function, defect dimensions may vary in length, width, area, and height. a′ is a test dimension, $\varphi(a)$ belongs to the normal distribution between

$$\mu(a') = \lambda_0 + \lambda_1\varphi(a') + \lambda_2\varphi^2(a') + \ldots + \lambda_m\varphi^m(a') \text{ and } \sigma^2,$$

that means

$$\varphi(a) \sim N(\mu(a'), \sigma^2) \quad (2)$$

in which the defect dimension a will have a′ value in nondestructive testing according to Eq 2. When $\varphi(a) = \ln a$, $\varphi(a') = \ln a'$, $m = 1$, substituting these values in Eq 1, one obtains

$$\ln a = \lambda_0 + \lambda_1 \ln a + \varepsilon\ \varepsilon \sim N(0, \sigma^2) \quad (3)$$

For discussion of Eq 3, uncertain parameters (λ_0, λ_1, and σ^2) were confirmed first, but discussion theory and method all can use Eq 1. If there are n defect numbers (a_1, a_2,. . ., a_n) that can be tested by nondestructive testing, comparison with the testing will give a_1', a_2',. . ., a_n' results. Based on regression analysis, the estimate value λ_0 and λ_1 are $\widehat{\lambda}_0$ and $\widehat{\lambda}_1$, the equation can be written

$$\widehat{\lambda}_0 = \overline{\ln a} - \widehat{\lambda}_1\overline{\ln a'};$$
$$\widehat{\lambda}_1 = \sum_{i=1}^{n}(\ln a - \overline{\ln a})(\ln a' - \overline{\ln a'}) \Big/ \sum_{i=1}^{n}(\ln a - \overline{\ln a})^2 \quad (4)$$

where $\overline{\ln a}$ is the real dimension average, and $\overline{\ln a'}$ is the test dimension average. Then

$$\overline{\ln a} = \tfrac{1}{n}\sum_{i=1}^{n}\ln a_i;\ \overline{\ln a'} = \tfrac{1}{n}\sum_{i=1}^{n}\ln a_i' \quad (5)$$

and the regression equation can be written as

$$\ln \widehat{a} = \widehat{\lambda}_0 + \widehat{\lambda}_1 \ln a' \quad (6)$$

and the unbiased estimator σ^2 is

$$\sigma^{2'} = \frac{1}{n-2}\sum_{i=1}^{n}\left(\ln a_i - \widehat{\lambda}_0 - \widehat{\lambda}_1 \ln a_i'\right)^2 \quad (7)$$

Model application. Table 6 shows the results of tomographic and visual defect area. The tomogram test showed a different area compared with the visual. Range of percentage difference between tomographic and visual defect area was 0.2-37.9%. Tomographic defect area was smaller than visual defect area except for disks 1, 9, and 15, which overestimated defect area. Decay area showed a larger percentage difference than void area. For example, percentage difference of disks 4, 5, and 10 were 22.0, 36.1, and 37.9%. However, results were not statistically significant enough to prove

Table 6. Results of tomographic and visual defect areas.

Disk no.	Diameter (cm)	Tomographic defect area (cm^2)	Visual defect area (cm^2)	Percentage difference (%)	Defect type
1	29.3	616.4	614.9	0.2	Void
2	20.7	150.4	186.2	19.2	Void
3	34.5	205.6	266.6	22.9	Void
4	28.3	86.7	111.1	22.0	Decay
5	29.9	48.0	75.1	36.1	Decay
6	32.9	43.3	50.2	13.7	Void
7	28.0	107.3	132.7	19.1	Void
8	30.2	44.0	51.9	15.2	Void
9	23.6	140.9	128.4	9.7	Decay
10	31.3	351.9	567.0	37.9	Decay
11	37.0	473.2	516.0	8.3	Void
12	22.6	156.7	192.5	18.6	Void
13	38.3	568.8	569.8	0.2	Void
14	37.4	540.8	616.6	12.3	Void
15	28.3	381.1	363.6	4.8	Void

tomographic decay area was more inaccurate than tomographic void area when using stress wave tomography to detect defect dimensions. Disk diameter did not significantly affect tomographic defect area when disk diameter ranged from 207-383 mm (Fig 3). Correlation of tomographic and visual defect area is shown in Fig 4. Although the tomogram test underestimated the defect area, the regression result showed excellent correlation between tomographic and visual defect area. The regression equation was $y = 1.0346x + 26.143$ (correlation coefficient was 0.9679). This regression result is useful for estimating cross-sectional defect area and decreasing the hazard assessment error ratio.

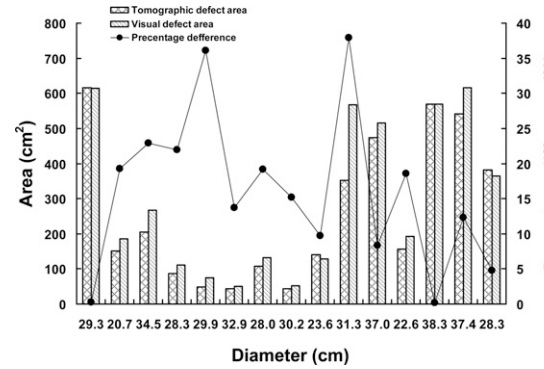

Figure 3. Comparison of tomographic defect area and visual defect area in disks 1-15.

Table 6 shows defect area results using SigmaScan Pro.5 software. The tomogram test showed a different area than the disk. Statistical analysis found the tomogram test area to be 86% of the real area when using 12 sensors (the tomogram defect area was smaller than the real defect area). The regression equation, an unbiased estimator between the real defect area ($\ln \hat{a}$) and the tomogram test defect area ($\ln a'$), can be calculated by Eqs 3, 4, 5, and 7. The equation is $\ln \hat{a} = 0.5018 + 0.9349 \ln a'$, and the unbiased estimator is $\sigma^2 = 0.1567$. This calculation method can be developed to estimate cross-sectional defect area when we know the tomogram defect area. It will decrease the hazard assessment error ratio by increasing defect area accuracy.

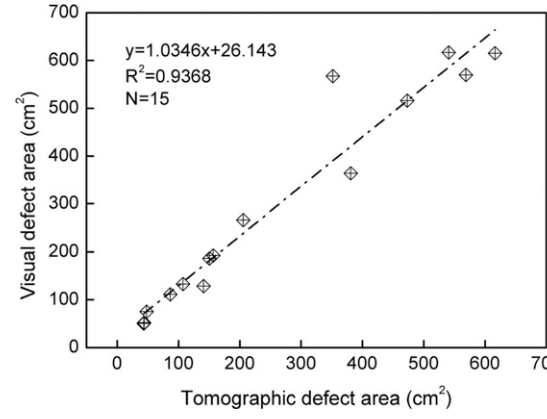

Figure 4. Linear regression of tomographic defect area and visual defect area in disks 1-15.

CONCLUSIONS

Stress wave tomography is effective at detecting existing defects in tree stems, although the technique cannot effectively distinguish decay or void by color change in tomograms (diagnosis of defect type is difficult). However, tomogram information can be used to assess stability of historic trees in combination with strength loss equations. Strength loss is a key index in assessing a tree's condition. Wagener, Coder, and Mattheck's equations were used to assess stem risk along with stress wave tomographic information. Results show that these equations can effectively assess tree trunk hazard. Mattheck's equation should be used to assess a tree's risk when the center of decay or void is not located in the center of the tree stem. The defect area predicted from a tomogram was underestimated compared with that derived from the disk. However, the regression result showed excellent correlation between tomographic and visual defect areas (correlation coefficient was 0.9679). There was a logarithmic relationship between real defect areas and defect areas indicated by the tomograms. This mathematical relationship could improve hazard assessment accuracy in old and famous urban historic trees when using stress wave tomography. Results of this research provide insight into defect diagnosis and hazard assessment of historic trees in China.

ACKNOWLEDGMENTS

The authors gratefully acknowledge financial support from the project Wood-inorganic Restoration Material (No. 2006-4-C03) in State Forestry Administration, P.R. China. We also greatly appreciate Mr. James H. Muehl for his comprehensive review, which enhanced this article.

REFERENCES

Allison RB, Wang XP, Ross RJ (2008) Visual and nondestructive evaluation of red pines supporting a ropes course in the USFS Nesbit lake Camp, Sidnaw, Michigan. Pages 43-48 *in* Proc 15th International Symposium on Nondestructive Testing of Wood, September 10-12, 2007, Madison, WI. Forest Products Society, Madison, WI.

Chinese National Standard (2009a) GB/T 1936.2-2009 Method for determination of the modulus of elasticity in static bending of wood. Standards Press of China, Beijing, China.

Chinese National Standard (2009b) GB/T 1936.1-2009 Method of testing in bending strength of wood. Standards Press of China, Beijing, China.

Chinese National Standard (2009c) GB/T 1940-2009 Method of testing in toughness of wood. Standards Press of China, Beijing, China.

Coder KD (1989) Should you or shouldn't you fill tree hollows. Grounds Maintenance 24(9):68-70, 98-100.

Comino E, Martinis R, Nicolotti G, Sambuelli L, Socco V (2000) Low current tomography for tree stability assessment. *In* GF Backhaus, H Balder, E Idczak, eds. International Symposium on Plant Health in Urban Horticulture, May 22-25, 2000, Braunschweig, Germany, 278 pp.

Divos F, Szalai L (2002) Tree evaluation by acoustic tomography. Pages 251-256 *in* Proc 13th International Symposium on Nondestructive Testing of Wood, August 19-21, 2002, Berkeley, CA. Forest Products Society, Madison, WI.

Fink GDS, Schwarze FWMR (2008) Detection of incipient decay in tree stems with sonic tomography after wounding and fungal inoculation. Wood Sci Technol 42:117-132.

Fu HM, Liu DD (1999) Fuzzy theory and application of nondestructive testing. J Aerospace Power 14(3): 225-230 [in Chinese].

Glibert EA, Smiley ET (2004) Picus sonic tomography for the quantification of decay in white oak (*Quercus Alba*) and hickory (*Carya* spp.). Journal of Arboriculture 30(5):277-280.

Mattheck C, Breloer H (1994) The body language of trees. A handbook for failure analysis. HMSO, London, UK. 240 pp.

Maurer H, Schubert SI, Baechle F, Clauss S, Gsell D, Dual J, Niemz P (2002) A simple anisotropy correction procedure for acoustic wood tomography. Holzforschung 60 (5):567-573.

Smiley ET, Fraedrich BR (1992) Determining strength loss from decay. Journal of Arboriculture 18(4):201-204.

Wagener WW (1963) Judging hazards from native trees in California recreational areas: A guide for professional foresters. Res. Paper PSW-RP-1. Pacific Southwest Forest and Range Experiment Station, Forest Service, U.S Department of Agriculture, Berkeley, CA. 29 pp.

Wang XP, Wiedenbeck J, LiangLiang SQ (2009) Acoustic tomography for decay detection in black cherry trees. Wood Fiber Sci 41(2):127-137.

Wang XP, Wiedenbeck J, Ross RJ, Forsman JW, Erickson JR, Pilon C, Brashaw BK (2005) Nondestructive evaluation of incipient decay in hardwood logs. Gen Tech Rep FPL-GTR-162. USDA For Serv Forest Prod Lab, Madison, WI. 11 pp.